

Promoter usage regulating the surface density of CAR molecules may modulate the kinetics of CAR-T cells *in vivo*

Jin-Yuan Ho,¹ Lin Wang,¹ Ying Liu,¹ Min Ba,¹ Junfang Yang,² Xian Zhang,³ Dandan Chen,¹ Peihua Lu,² and Jianqiang Li¹

¹Hebei Senlang Biotechnology, Shijiazhuang 050000, China; ²Hebei Yanda Lu Daopei Hospital, Langfang, China; ³Hebei Yanda Lu Daopei Hospital, Beijing, China

Although chimeric antigen receptor T (CAR-T) cell therapy achieves high remission rates, challenges (e.g., toxicity management and relapse prevention) remain. The major risks are cytokine release syndrome and related neurological toxicity. The influence of the CAR surface density on the efficacy/safety of CAR-T cell therapy and the factors determining CAR density were not elucidated comprehensively. Here, we discovered that the use of the MND promoter increased the transduction rate and reduced the CAR surface density. Additionally, MND-driven CAR-T cells had prolonged antileukemia activity in a mouse model. In an initial dual-armed anti-CD19 CAR-T cell pilot study (ClinicalTrials.gov: NCT03840317), eight and six subjects were infused with MND and EF1 α promoter-driven autologous CAR-T cells (3×10^5 CAR-T cells/kg), respectively. MND subjects developed mild fever and lower interferon gamma (IFN- γ) concentrations than in the EF1A19 group. All but one subject in each cohort reached minimal residual disease (MRD)-negative complete remission after the first month of evaluation. These results represent the first comprehensive study on the promoter-driven modulation of CAR-T cell functionality. These findings encourage further evaluation of the potential of the MND promoter to drive CAR-T cells as a broadly applicable cellular product for anticancer immunotherapy.

INTRODUCTION

Anti-CD19 chimeric antigen receptor T (CAR-T) cell therapy is highly effective in the treatment of relapsed or refractory acute B cell leukemia (B-ALL)^{1–3} and diffuse large B cell lymphoma (DLBCL).^{4–6} However, there are limitations due to safety issues, including cytokine release syndrome (CRS) and neurotoxicity (CAR-related encephalopathy syndrome, CRES).^{7,8} However, safety and effectiveness often occupy opposite ends of the seesaw, and it is pivotal to determine the optimal balance to achieve the best result. A recent study revealed that novel CAR-T cells carrying low-affinity anti-CD19 scFv effectively exerted antileukemia activity and reduced the degree of toxicity in patients.⁹ In addition to examinations of affinity modulation, evidence showed that the surface density of the target antigen may affect the response strength of CAR-T cells, which changes the efficacy and

safety.¹⁰ Lower surface antigen density resulted in lower cytokine production by CAR-T cells. Previous studies indicated that toxicity was directly related to CAR-T cell cytokine production.^{11,12} However, one study showed that the antigen surface density threshold required for cytokine production was 10-fold higher than the density required for lytic activity.¹³ These results provide a hint for solving the dilemma of safety and efficacy by exploiting the density issue.

There are several different strategies to engineer T cells, including lenti/retroviral-vector-based transfer and direct DNA/mRNA transfer via electroporation. Lentiviral transfection was used in most studies, including the marketed product Kymriah. The elongation factor 1 A (EF1A) promoter is a strong promoter in various cell types, and it is used to drive most CAR expression. A recent study considered promoter choice when a long and complicated mRNA was used in gene therapy.¹⁴ Four promoters, EF1A, CMV, hPGK, and RPBSA, were used to compare the packaging and transduction efficiencies, marker and CAR expression, cytokine production levels, and lytic abilities, and EF1A was best of these four promoters. However, MND (myeloproliferative sarcoma virus MPSV enhancer, negative control region NCR deletion, d1587rev primer binding site replacement) had good transcriptional ability in cancer cells in a 1997 study.¹⁵ Further studies also revealed that use of the MND promoter promoted high transduction efficiency and expression levels in murine and mammalian hematopoietic stem cells.^{16–19}

As mentioned above, the density of antigen modulates CAR-T cell functionality. Therefore, the density of CAR molecules on CAR-T cells may also modulate the nature of the antitumor activity. Previous studies compared the transduction efficiency of the EF1 α and MND promoters,^{20,21} but there are no reports on the density of the target protein and the corresponding cell functionality. We hypothesize

Received 15 November 2020; accepted 8 March 2021;
<https://doi.org/10.1016/j.omtm.2021.03.007>.

Correspondence: Jianqiang Li, Hebei Senlang Biotechnology, Runjiang Headquarters International, Building No. 6, Shijiazhuang 050000, Hebei, China.
E-mail: lijianqiang@senlangbio.com

Correspondence: Pei-hua Lu, Hebei Yanda Lu Daopei Hospital, Sipulan Road No. 6, Yanjiao, Langfang, Hebei, China.

E-mail: peihua_lu@126.com



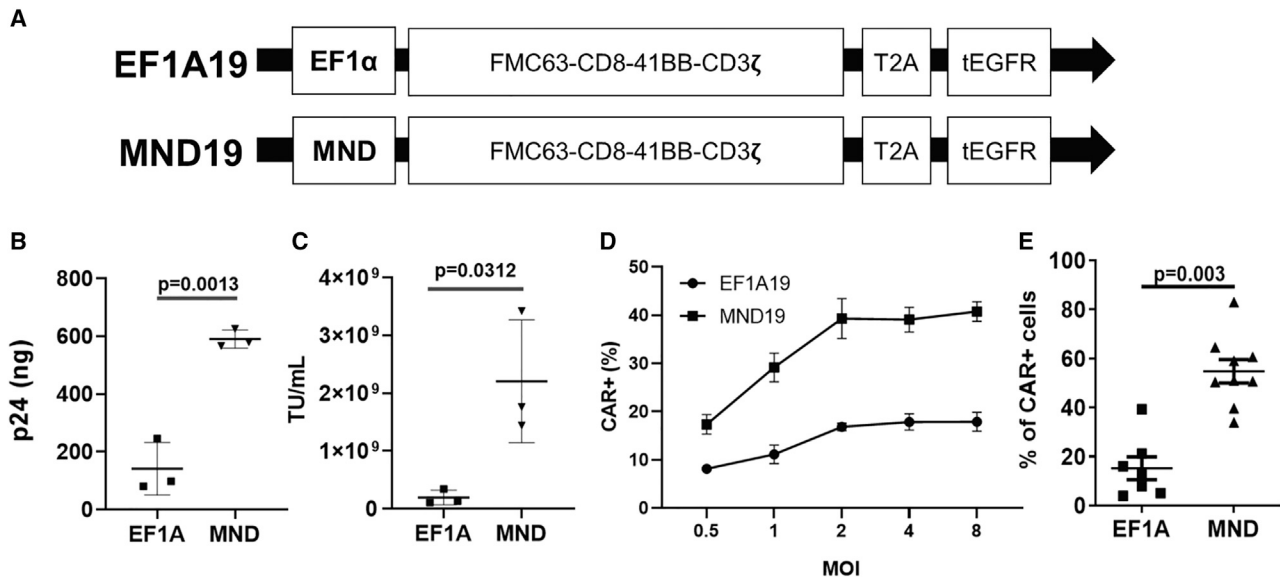


Figure 1. Schematic of the CAR and the features of the MND and EF1A lentiviruses

(A) Schematic of the recombinant anti-CD19 CAR with the EF1 α or MND promoter. (B) Package efficiency of the two lentiviral vectors was determined by the concentration of HIV p24 in the supernatant (n = 3). (C) The transfection titer of the lentiviral vectors was estimated via transduction into K562 cells and assessment using flow cytometry (n = 3). (D) Transduction efficiency of the two lentiviral vectors by MOI (day 6, n = 3). (E) Transduction rates of EF1A (n = 7) and MND (N = 9) lentiviral vectors on CD3⁺ T cells from different donors (MOI = 1). The results are expressed as the mean \pm SEM.

that the MND promoter would affect the transduction efficiency and changes the surface density of CARs, which would alter CAR-T functions. The present study compared the *in vitro* and *in vivo* activities of these two CAR-T cells and initiated a pilot study to examine the effects of CAR molecule density on the safety of CAR-T cells. To our knowledge, this report is the first study to investigate the safety and efficacy of MND-driven CAR-T cells.

RESULTS

Lentiviruses with the MND promoter have increased packaging efficiency and dramatically increase the percentage of CAR-positive cells

To study the effect of promoter usage on the functions of CAR-T cells, two plasmids, EF1A19 (EF1A) and MND19 (MND), were generated with the EF1 α and MND promoters, respectively (Figure 1A). Except for the different promoters, the remaining components of the CAR structure were identical, including an FMC63 scFv, a CD8-derived hinge and transmembrane domain, a 4-1BB signal domain, a CD3-zeta signal domain, and a C-terminal truncated epidermal growth factor receptor (tEGFR). We packaged these two lentiviruses using third-generation lentivirus packaging system. We observed the effect of different promoters on the features of the packaged lentiviral vectors. The physical and infectious titers of the packaged vectors were determined using ELISA and flow cytometry (infected HEK293FT cells). As shown in Figure 1B, the physical titer of MND19 was 590.372 ± 18.084 ng/mL, which was significantly higher than EF1A19 at 141.267 ± 52.602 ng/mL ($p = 0.0013$). The infectious titer of MND19 was $2.21E9 \pm 6.14E8$ transduction units (TU)/mL, compared to

$1.95E8 \pm 7.34E7$ TU/mL for the EF1A19 vector ($p = 0.0312$) (Figure 1C). The transduction efficiency of the two lentiviral vectors in CD3⁺ T cells under the same conditions was determined using biotin-labeled Erbitux and flow cytometry.²² As shown in Figure 1D, the mean percentage of MND19 CAR-T cells increased with the increase in the multiplicity of infection (MOI) from 17.37% to 39.3% (MOI 0.5, 1, and 2, respectively). However, a further increase in MOI did not increase the mean transduction rate of CAR-T cells (MOI = 4 and 8 for 39.1% and 40.77%). Similar to MND19, the increase in MOI did not increase the mean value of transduction rate of the EF1A19 lentiviral vector. The transduction rates for EF1A19 at all the tested MOIs were 8.16%, 11.15%, 16.83%, 17.9%, and 17.37%.

This observation was further validated by examining the transduction efficiency from several batches of EF1A19 and MND19 lentiviral vectors. As shown in Figure 1E, the average transduction rates of EF1A19 and MND19 were $15.22\% \pm 4.64\%$ and $57.77\% \pm 4.80\%$ ($p = 0.003$), respectively. These results indicated that MND19-transduced CAR-T cells may have a higher transduction efficiency.

MND19 has a lower MFI value than EF1A19 when the surface CAR molecule was labeled with either CD19-Fc protein or anti-FMC63 scFv

Unexpectedly, our analysis of the transduction efficiency of these two vectors revealed that the mean fluorescence intensity (MFI) seemed higher in MND19 CAR-positive cells than in EF1A19 CAR-positive cells (Figure S1A). To further confirm this observation, Erbitux, CD19Fc, and an FMC63 scFv-specific idotype antibody (aFMC63)

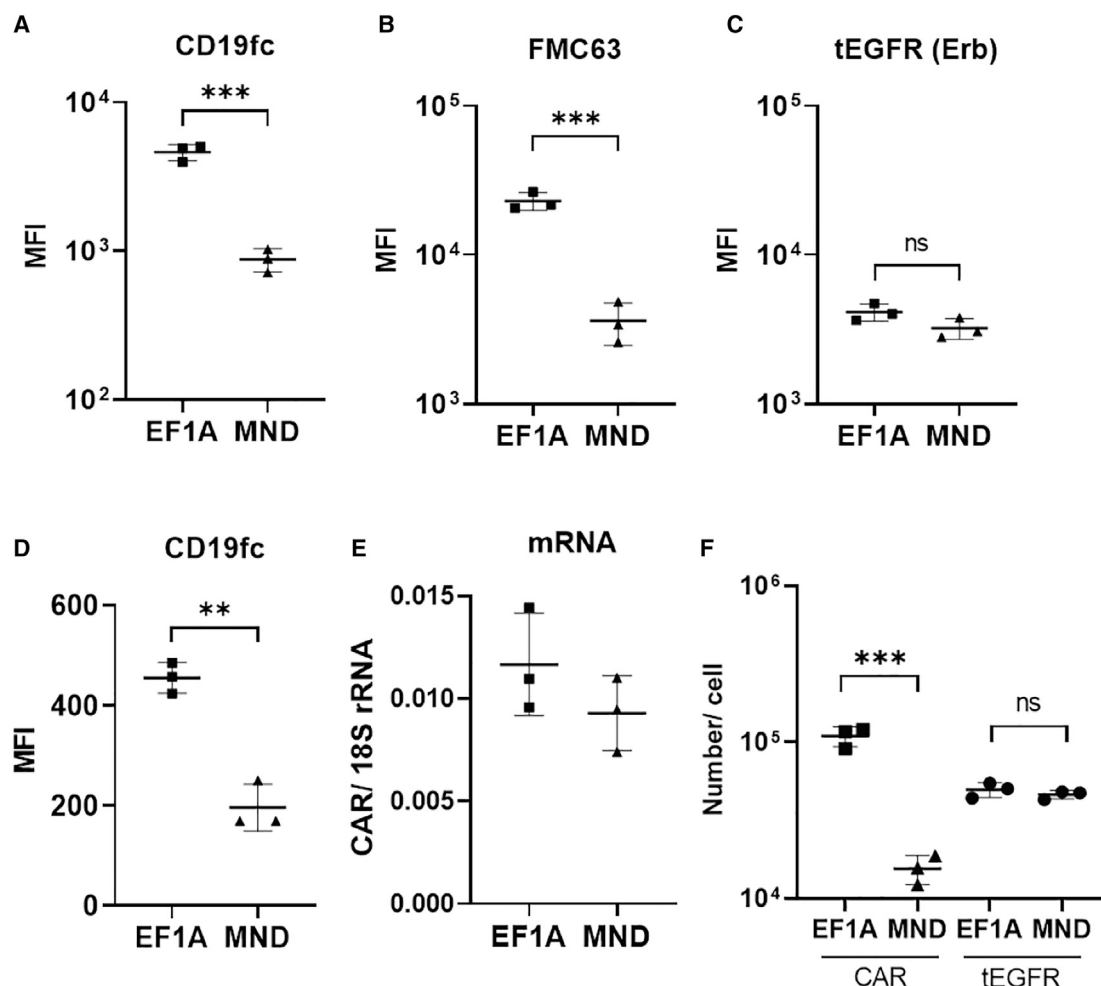


Figure 2. Density and surface number of CAR molecules

(A–C) The MFI of the CAR molecules as determined by (A) CD19Fc, (B) anti-FMC63 idiotype antibody, and (C) the transduction marker tEGFR using flow cytometry and FlowJo 10 analyses. The results are expressed as the mean \pm SD. (D) The MFI of the CAR molecules determined by CD19Fc on day 12. (E) The relative expression level of CAR and 18S rRNA (after tEGFR enrichment on day 16). (F) Number of CAR molecules on the surface estimated using an ABC assay. ns, nonsignificant; * $p < 0.05$; ** $p < 0.01$; *** $p < 0.001$.

were used to simultaneously examine the expression of tEGFR and CAR on the surface of CAR-T cells. As shown in Figures 2A and 2B, the expression of the CAR driven by the MND promoter was significantly lower than the CAR driven by the EF1A19 promoter on day 6 after manufacture (transduction day 2), as determined using CD19Fc (876 ± 156.2 versus $4,621 \pm 576.4$, $p = 0.0004$) or the idiotype antibody against FMC63 scFv ($3,606 \pm 1,140$ versus $22,920 \pm 3,083$, $p = 0.0005$).

Notably, we found that the expression of tEGFR on CAR-T cells was not consistent with the expression of CAR. There was no significant difference in tEGFR between EF1A19 and MND19 CAR-T cells, and the MFIs were $4,127 \pm 549.2$ versus $3,216 \pm 509.4$ ($p = 0.1029$) using Erbitux staining (Figure 2C). We examined whether this observation was a transient phenomenon and continually examined the MFI on day 12 after CAR-T cell manufacture. The MFI of CAR remained

significantly lower on MND19 CAR-T cells, which was similar to day 6 (Figures 1D and S1B). We examined the mRNA expression of these two CAR-T cells on day 14. As shown in Figure 2E, the expression level was slightly lower in enriched MND19 CAR-T cells, but there was no significant difference between EF1A19 and MND19 CAR-T cells.

MND promoter reduced the density of CD19 CAR molecules on the cell surface

MFI measurements are related to affinity or avidity. Because the same CAR construct was used in EF1A19 and MND19 CAR-T cells, the affinity should be similar. Therefore, we questioned whether different promoters changed the surface density of CAR and tEGFR. The number of CAR molecules and tEGFRs on the surface of these two CAR-T cell types was measured using an antibody-binding capacity (ABC) bead assay.²³ Four standard microbeads with known

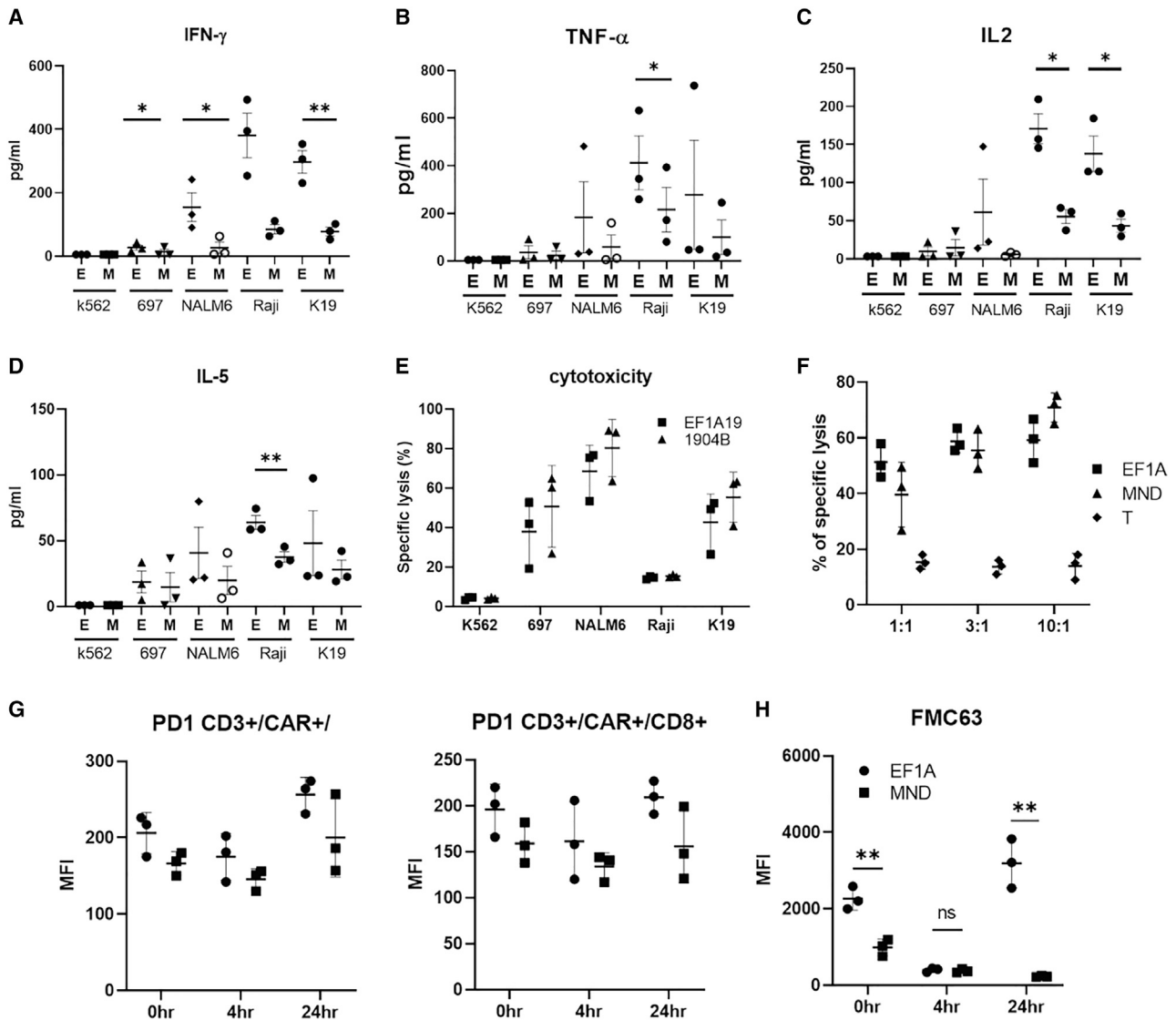


Figure 3. Reduced cytokine secretion by MND-driven anti-CD19 CAR-T cells

(A–D) IFN- γ (A), TNF- α (B), IL-2 (C), and IL-5 (D) release profiles of EF1A and MND CAR-T cells targeting CD19-positive cancer cell lines (K562, 697, NALM-6, Raji, and K562-CD19) at a 3:1 E:T ratio ($n = 3$). (E) Specific lysis by EF1A and MND CAR-T cells targeting CD19-expressing cancer cell lines at a 3:1 E:T ratio ($n = 3$). (F) Specific cell lysis of K562-CD19 cells by EF1A, MND, and untransduced T cells at different E:T ratios ($n = 3$). (G) The MFI of PD1 on CD3⁺/CAR⁺ and CD3⁺/CAR⁺/CD8⁺ cells. (H) The MFI of CAR before and after NALM-6 coculture (E:T, 1:1). The results are expressed as the mean \pm SD. ns, nonsignificant; * $p < 0.05$; ** $p < 0.01$; *** $p < 0.001$.

antibody-binding capacities were labeled with CD4-fluorescein isothiocyanate (FITC), and flow cytometry was used to obtain a standard curve (Figures S2A–S2C). The number of CAR molecules on the surface of EF1A19 and MND19 CAR-T cells was $109,426 \pm 15,911$ and $15,542 \pm 3,241$ ($p = 0.0006$) per cell, respectively (Figure 2F). The number of tEGFRs was $49,659 \pm 5,404$ and $46,140 \pm 2,883$ ($p = 0.376$) for EF1A19 and MND19, respectively (Figure 2F).

We further used the MND promoter with other CAR constructs and found that a reduction in CAR surface density was also observed in MND-BCMA compared to EF1A-BCMA (Figure S2D).

MND19 cells secrete fewer cytokines than EF1A19 cells without reducing cytotoxicity

A previous study showed that the density of the target antigen on the cell surface changed the CAR-T cell response.¹⁰ We wondered whether a decrease in the CAR surface density would change the functionality of the T cells. We evaluated cytokine release targeting CD19-positive cell lines *in vitro*. CD19-positive cell lines (697, Raji, NALM6, and K562-CD19) were cocultured with CAR-T cells at an effector/target (E:T) ratio of 3:1. The site density of CD19 on these cells was assessed using flow cytometry (data not shown), and the MFI values were 1,829, 4,253, 5,184, and 6,129, respectively. Notably, MND19 CAR-T cells produced

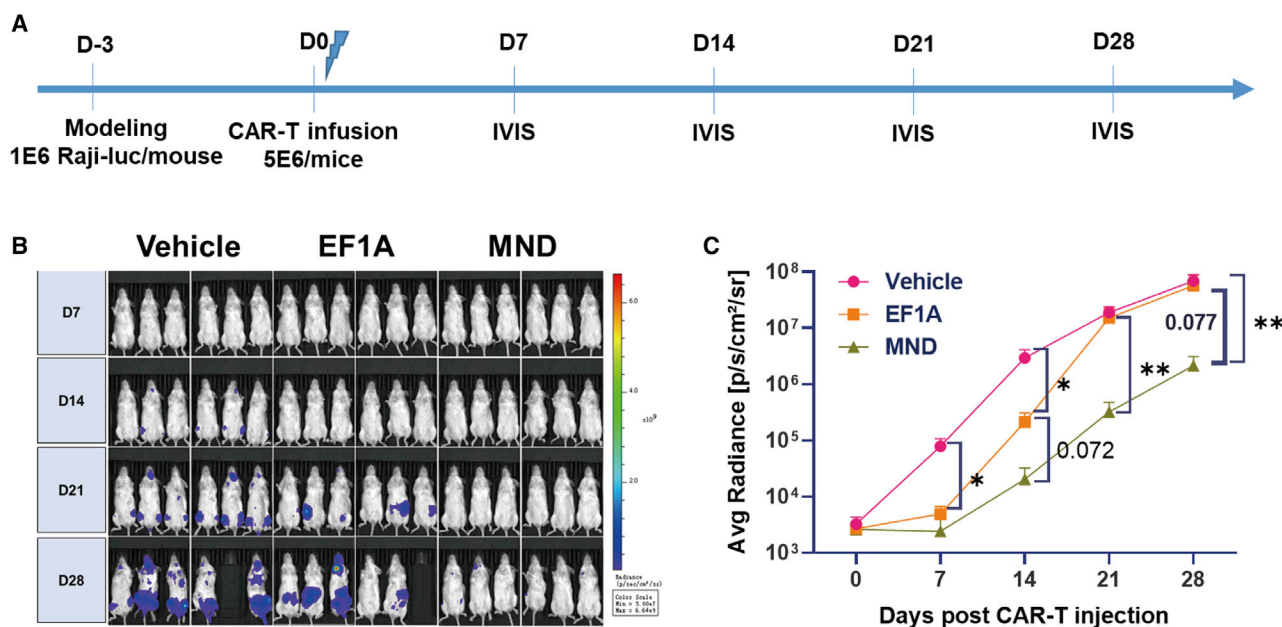


Figure 4. MND19 CAR-T cells have better antileukemia activity in the Raji mouse model

(A) *In vivo* experimental design of the tumor engraftment, CAR-T cell treatment, and observation timeline. First 1E6 Raji cells were infused into NOD/SCID mice. (B and C) The mouse model demonstrated the antileukemia effect of MND CAR-T cells by the BLI of the transplanted mice ($n = 6$). The results are expressed as the mean \pm SEM. ns, nonsignificant; * $p < 0.05$.

lower amounts of cytokines (Figures 3A–3D; Table S1). We next examined whether the cytotoxic activity was also diminished as cytokine release was reduced. As shown in Figure 3E, MND19 CAR-T cells showed similar cytotoxic activity as the EF1A19 CAR-T cells. We further investigated the cytotoxicity at different E:T ratios, targeting K562-CD19. As shown in Figure 3F, there was no significant difference between EF1A19 and MND19 CAR-T cells targeting K562-CD19 at E:T ratios of 1:1, 3:1, or 10:1. These results suggested that the reduction in CAR surface density at certain levels only affected cytokine release but not cytolytic activity. These results are consistent with a previous study,¹³ in which the antigen density required for cytokine production was 10-fold higher than the density required for cytolytic activity. This effect was applicable to the antigen density and the CAR density.

We also investigated T cell exhaustion and CAR recovery upon antigen stimulation. The expression of PD1 before (0 h) and after antigen stimulation (4 h and 24 h) was lower on MND19 CAR-T cells than their EF1A19 counterparts (Figures 3G and S3A). The density of CAR was significantly reduced on both CAR-T cells 4 h after stimulation. The density of CAR recovered on EF1A19 CAR-T cells at 24 h but not on MND19 CAR-T cells.

Raji modeling with NOD/SCID mice demonstrated that MND19 has better *in vivo* antitumor efficacy

In vitro studies showed that MND19 CAR-T cells exerted the same cytolytic activity with reduced cytokine production. We examined whether reduced cytokine production by MND19 CAR-T cells diminished CAR-T cell activity *in vivo*. To compare the antileukemia activities of

EF1A19 and MND19 CAR-T cells, a Raji cell-derived xenograft model was established in non-obese diabetic (NOD)/severe combined immunodeficiency (SCID) mice via the intravenous infusion of 5E6 CAR-T cells per mouse (Figure 4A). As shown in Figure 4B, one mouse in the vehicle group died on day 24, and another mouse in the EF1A group died on day 28. No other mice died during the 28 days of observation, and no signs of graft-versus-host disease (GVHD) were observed (Figure S4A). Bioluminescence imaging (BLI) results revealed that tumor cell proliferation was initially significantly suppressed in mice treated with EF1A19 and MND19 CAR-T cells (Figure 4C, days 7 and 14). However, the inhibitory effect of EF1A19 CAR-T cells was reduced after day 21, but the antileukemia activity of MND19 CAR-T cells was sustained until day 28 (Figure 4C, days 21 and 28).

To further examine the safety and efficacy of MND19 CAR-T cells, we evaluated MND19 CAR-T cells in another Raji mouse model (B-NDG), which has the same phenotype as NSG mice. As shown in Figure S4B and S4C, mice in the vehicle group all died within 14 to 16 days. (Raji cells were inoculated on day –3). The median survival times for vehicle, T cell, 5E6 and 1E7 CAR-T cells, and the negative control were 14.5, 36, 47.5 and 90<, and 90< days, respectively. No signs of GVHD were observed. These results support the safety and efficacy of MND19 CAR-T cells in a mouse model.

A pilot study revealed the potential safety benefit of MND19 CAR-T cells

Based on the above studies, we hypothesized that MND19 CAR-T cells would produce lower levels of cytokines *in vivo* than EF1A19

Table 1. Subject demographics

	Cohort A (N = 6)	Cohort B (N = 8)	p value
Age, median (range)	9 (3–31)	23.5 (4–38)	0.17
Male/female	3/3	5/3	0.67
Weight, kg, median (range)	28 (18–62)	54 (16–101.5)	0.07
Prior treatment, median (range)	9 (3–15)	6 (4–12)	0.38
BM blasts, %, median (range)	3 (0.68–82.68)	4.49 (1.29–39.04)	0.38
Dose	3×10^5 /kg	3×10^5 /kg	

CAR-T cells and the corresponding severity of CRS would be lower than that with EF1A19 CAR-T cells. A randomized, double-blinded, single-center pilot study was initiated on patients with relapsed and refractory acute B-ALL to compare the safety and efficacy of EF1A19 and MND19 CAR-T cells (NCT03840317). Eighteen patients were screened from November 2018 to November 2019, and 15 of these patients were enrolled and randomly assigned into cohort A (EF1A19) and cohort B (MND19), which contained 7 and 8 subjects, respectively (Figure S5A). Table 1 compares the subject demographics, and there were no significant differences in the subjects' baseline parameters (Table S2) or the characteristics of the CAR-T cells, including the T cell phenotypes and the percentage of PD1 expression (Figure S5B). The median follow-up days for the EF1A19 and MND19 cohorts were 226 and 233 days (ranging from 134 to 291 days and 152 to 297 days), respectively.

The primary efficacy and safety evaluations were performed on day 28 post-infusion. All subjects in cohort B (MND19) reached complete remission (CR), and seven of them (7/8) were minimal residual disease (MRD) negative (Table 2). Five of the six subjects in cohort A (EF1A19) reached MRD-negative CR, and the other subject had disease progression. The treatment responses of each subject are depicted in Figure 5A. After CAR-T-induced CR, all subjects but one (12/13) received allogeneic hematopoietic stem cell transplantation (allo-HSCT), and the median time from the day 28 evaluation to allo-HSCT was 31 days (14–106 days) and 24.5 days (13–42 days) for cohorts A (EF1A19) and B (MND19), respectively. Two of the subjects in cohort B (MND19) who bridged to allo-HSCT eventually relapsed. Adverse events related to CAR-T cell therapy were recorded (Table S3), and most subjects experienced mild CRS. Two subjects in each group experienced CRS \geq grade 2, and one subject in cohort B (MND19) experienced grade 3 CRES, which was later relieved with dexamethasone and tocilizumab administration (Table S2). This pilot study suggested that MND19 CAR-T cells and EF1a promoter-driven anti-CD19 CAR-T cells exerted antileukemia activity. Due to the sample size, there were no significant differences between these two products in CRS or CRES occurrence or the CR rate (Table 2).

Although the outcomes and safety were not significantly different in this small pilot study, several interesting trends were observed. First, body temperature elevation seemed mild in subjects infused with MND CAR-T cells (Figure 5B), and the peak body temperature of each subject was lower in the MND cohort (Figures S6A and S6B).

Table 2. Summary of safety and efficacy

	Cohort A (N = 6)	Cohort B (N = 8)	Significance
CRS, grade \geq 2	33.3% (2)	25% (2)	NS
CRES, grade \geq 2	0% (0)	12.5% (1)	NS
Dexamethasone	1	2	
Tocilizumab	1	1	
CR	83.3% (5)	100% (8)	NS
MRD, +	0% (0)	12.5% (1)	
Median OS, days	Not reached	324	
Median PFS, days	Not reached	Not reached	

CRS, cytokine release syndrome; CRES, CAR-T cell-related encephalopathy syndrome; CR, complete remission; MRD, minimal residual disease; OS, overall survival; PFS, progression-free survival; NS, not significant.

The absolute number and percentage of CAR-T cells in peripheral blood peaked on day 10 (Figures 5C and S6C–S6F). The expansion of MND19 CAR-T cells was slower than EF1A19 CAR-T cells on day 7 (Figure S6F), but the kinetic curve of MND19 was similar to EF1A19 after day 10. There were no significant differences in interleukin-4 (IL-4), IL-10, interferon gamma (IFN- γ), or IL-6 during the 28 days of observation (Figure S6G).

DISCUSSION

The functionality of CAR-T cells depends on the interaction between the tumor and T cells. A previous study showed that the threshold of the target antigen required to activate CAR-T cells was 10 times higher for the release of cytokines than for exerting cytolytic activity.¹³ These findings are supported by Fry et al.,¹⁰ who demonstrated that lower CD22 surface density resulted in lower cytokine release upon CAR-T cell treatment. Scientists also developed a universal CAR-T cell therapy using CRISPR-Cas9 to engineer CAR into the T cell receptor alpha chain (TRAC).^{24,25} Eyquem et al.²⁵ revealed that higher CAR expression by TRAC-EF1 α -1928z than TRAC-1928z did not produce better antitumor activity. They also found that TRAC-1928z prevented tonic CAR signaling and reduced exhaustion marker expression. Therefore, a lower CAR surface density would impede spontaneous tonic signaling. Consistent with these results, our findings suggested that a lower level of CARs on the cell surface may also reduce cytokine release without reducing the antitumor activity of CAR-T cells.

The influence of surface CAR expression on different promoter-driving CARs was also investigated by Guedan et al.²⁶ These authors compared pGK300-BBz with EF1A-BBz (pGK300 is a truncated promoter of phosphoglycerate kinase). Notably, pGK300-BBz exhibited reduced surface CAR density, barely eradicated the inoculated tumor cells, and the antitumor activity was much lower than EF1A-BBz. These results are unlike the MND promoter in our study, which retained a similar antitumor activity *in vitro* and *in vivo*. This result may be due to the insufficiency of CAR/antigen interactions to reach the threshold for activation of the cytolytic activity of T cells, as

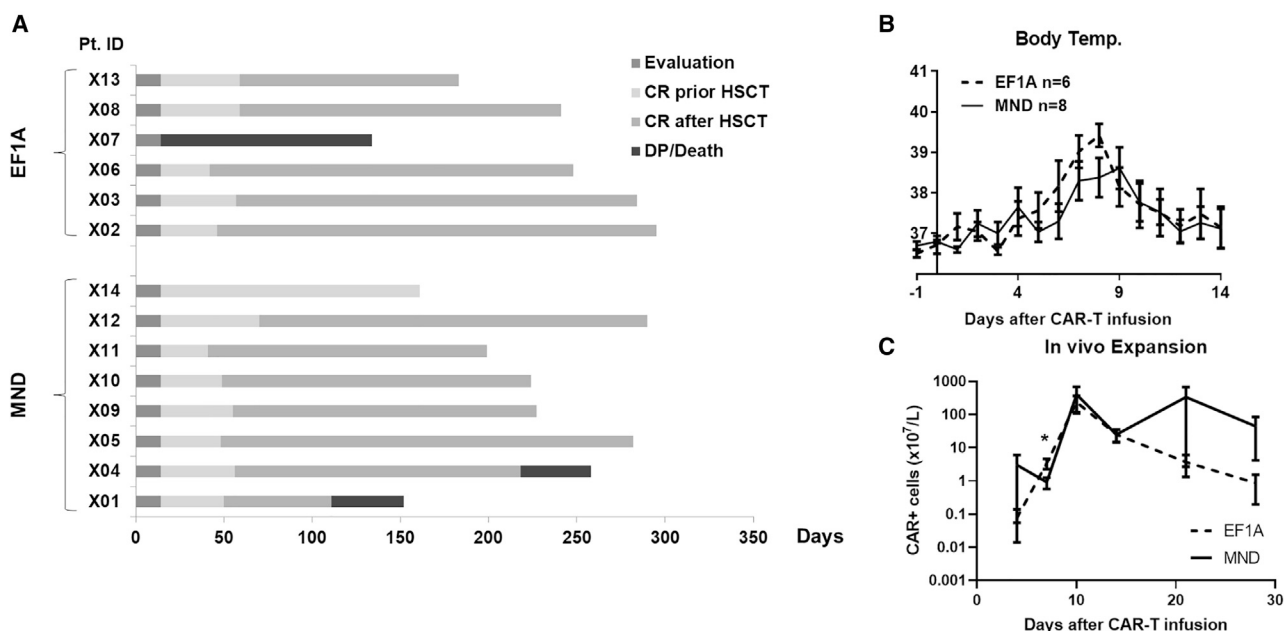


Figure 5. Infusion of MND CAR-T cells reduced the severity of CAR-related adverse effects, but the efficacy was retained

(A) Swimmer plot of enrolled subjects. CR, complete remission; HSCT, haploid hematopoietic stem cell transplant; DP, disease progression. (B) The dynamics of daily peak temperature. (C) Expansion of CAR-T cells *in vivo* estimated by the complete blood count and percentage of CAR-T cells in the peripheral blood. The results are expressed as the mean \pm SEM.

discussed by Watanabe et al.¹³ Other reasons, such as the characteristic difference between blood tumors and solid tumors and the antigen density on the tumor cells (K562-CD19 and capan-2), cannot be excluded.

One recent study compared the lentiviral titer, transduction efficiency, marker and CAR expression levels, cytokine production (IL-2 and IFN- γ), and killing ability of four promoters, including EF-1 (EF-1A in our study), CMV, hPGK, and RPBSA.¹⁴ EF-1 exhibited the best transduction efficiency, killing ability, and cytokine production. Consistent with our observations, these authors observed a reduction in CAR expression driven by the hPGK and RPBSA promoters, which retained acceptable killing ability but reduced cytokine production. However, we observed that the MND promoter enhanced the packaging efficiency, which was consistent with the suggestion that different promoters resulted in different lentiviral titers.

We next investigated the mechanisms that led to the inconsistent expression of CAR and tEGFR. Although the mRNA expression level was slightly lower on MND19 CAR-T cells (Figure 2E), we do not know whether such a mild difference would be augmented during the translational process. However, two proteins linked by the 2A sequence should be equally expressed. A previous study revealed a phenomenon in which protein expression after the 2A sequence was higher than expression before the 2A sequence, which was only observed by T2A but not by P2A.²⁷ Therefore, the choice of promoter and T2A together may explain this observation.

Our preclinical study did not observe a significant difference in survival rates over the 28 days of observation (Figure 4B). An early report revealed that the use of NOD/SCID mice with IL2R gamma (null) (NSG) instead of NOD/SCID mice may shorten the time required for tumor engraftment.²⁸ Therefore, the survival of mice in the vehicle group may have been due to the use of NOD/SCID mice. However, EF1A19 CAR-T cells seemed less effective on days 21 and 28 in this model (Figure 4C), which may raise concerns about the efficacy of EF1A19 CAR-T cells. However, EF1A19 CAR-T cells were indeed as effective as MND19 CAR-T cells in the *in vitro* and human pilot studies, which suggested that the EF1A19 CAR-T cells used in the present study did not differ from other reported anti-CD19 CAR-T cells. The observation of reduced antileukemic activity may also be related to the mouse model. The NOD/SCID animal model seemed to distinguish minor differences between two CAR-T cells, but whether such a small change is observable in the NSG model remains to be clarified.

In summary, we demonstrated a higher packaging efficiency but reduced density of surface CAR molecules when using MND, rather than EF1 α , as the promoter. The reduced surface density of CAR molecules did not affect *in vitro* or *in vivo* cytotoxicity, but it may lead to lower cytokine release. This finding suggests that altering the avidity between the target and scFv is simplified with the use of another promoter. The present study suggests that surface CAR density on T cells modulates efficacy and safety. A possible mechanism for this observation was not elucidated, and further investigation is required to understand how different promoters affect the density of CAR molecules

on the cell surface. Due to the small sample size, we cannot conclude any significant benefit of MND19 CAR-T cells, but the results are encouraging and deserve further investigation.

MATERIALS AND METHODS

Cells (tumor cells and peripheral blood mononuclear cells)

K562 (ATCC_CCL-243), K562-CD19, 697 (DSMZ_ACC 42), NALM-6 (DSMZ_ACC 128), and Raji/ffluc cells were cultured in RPMI-1640, 10% fetal bovine serum (FBS, ExCell Bio, FND500, China), and 100 U/mL penicillin/streptomycin. K562 cells were transduced with genes encoding human CD19, and the positively transduced K562-CD19 cells were selected with puromycin. The absence of mycoplasma was confirmed for all cell lines by monthly testing. Peripheral blood mononuclear cells were isolated from the blood of healthy donors or from the apheresis of enrolled patients. T cells were isolated and cultured as described previously.²⁹

Lentiviral vector construction and virus preparation

Sequences encoding human anti-CD19 scFvs (FMC63) were linked to a CD8 hinge and transmembrane region, a 4-1BB-derived costimulatory domain, and intracellular CD3 ζ . The CAR gene was combined with a sequence encoding EGFRt by a T2A sequence and cloned into the lentiviral vector pLenti. The EF1 α promoter was substituted with the MND promoter by overlapping PCRs to generate the 1904 construct. The vector with the MND promoter was further named MND19, and the vector with the EF1 α promoter was named EF1A19.

Lentiviruses were packaged via transient transfection of HEK293FT cells using pRSV, pMDLg, pMD2.G, and MND19/EF1A19 with polyethylenimine. After 48 h of incubation, the supernatant was collected for p24 determination using ELISA (Takara, #632200). Supernatants were further centrifuged for 2 h at 20,000 \times g, and the pellet was suspended in TexMACS, aliquoted and stored at -80°C . The TUs of EF1A19 and MND19 were determined using flow cytometry. Briefly, various amounts of virus were used to transduce K562 cells. After 72 h of transduction, transduced K562 cells were labeled with biotinylated Erbitux to identify the percentage of CAR-positive cells. The TU/mL was calculated as 1×10^6 cells \times % (of CAR⁺) \div volume of virus (μL) \times 1,000.

Flow cytometry

Tumor cells and T cells were phenotyped with CD3-APC (OKT3, UCH1), CD19-APC Cy7 (SJ26C1), CD4-PE Cy7 (RPA-T4, A161A1), CD8-Pacific blue (RPA-T8, SK1), streptavidin-APC-Cy7 (405208), PD1-FITC (329904), TIM3-PE (345006), LAG-3-APC (369212), APC-Annexin V (640920), and 7AAD (420404), which were purchased from Biolegend (London, UK). Antibiotin-PE was purchased from MACS (Miltenyi Biotec, Germany). CD19Fc-FITC (CD9-HF251) and BCMAFc-FITC (BC7-H5254) were purchased from Acro (Acro, USA). Anti-FMC63 scFv-APC (R19PB-100) was purchased from Bioswan. The percentages of CD19 CAR⁺ T cells were determined using flow cytometry after staining with Erbitux (Roche, USA).²² Data acquisition was performed on a MACSquant

10, and the results were analyzed using FlowJo software version 10 (Tree Star).

Transduction of T cells and *in vitro* functional assays

Primary human T cells were activated, transduced, enriched, and expanded as described previously.²⁹ In brief, peripheral blood mononuclear cells were selected using CD3 microbeads (Miltenyi Biotec: 130-050-101) and then activated with CTS CD3/CD28 Dynabeads (GIBCO: 40203D). T cells were cultured in 200 IU of IL-2-supplemented TexMACS (Miltenyi Biotec: 170-076-309) for 2 days. T cells were transduced with MND19 and EF1A19 separately in the presence of 8 ng/mL protamine sulfate. The transduction rate of CAR-T cells was determined on day 5 or 6 using flow cytometry 3 to 4 days after transduction. CAR-T cells were expanded in TexMACS with 200 IU of IL-2 until day 14.

Cytotoxicity was analyzed in a 4-h coculture of effector and target cells. All of the target cells were first incubated with carboxyfluorescein succinimidyl ester (Biolegend: 423801) before coculture with MND19 or EF1A19 CAR-T cells. Four hours after coculture, all cells were collected for Annexin V and 7AAD staining. The specific cytotoxicity was calculated as 100% minus the percentage of Annexin V and 7AAD double-negative cell populations. Cytokine concentrations were determined using a 14-cytokine detection kit (QuantoBio, Tianjing, China: C60011) as previously described.²⁹ The MFI of PD1, LAG3, and TIM3 was determined before and after NALM-6 coculture on day 16.

Measurement of mRNA expression

CAR⁺ cells of MND19 and EF1A19 were labeled with biotinylated-Erbitux prior to the selection using streptavidin Microbeads (Miltenyi: 130-048-101) per the manufacturer's instruction. The mRNA was extracted from CAR⁺ cells using an RNAPrep pure Cell/Bacteria Kit (Tiangen, China: DP430) according to the manufacturer's instructions, and then the mRNA was reversely transcribed into cDNA using a FastQuant RT kit (Tiangen: KR106-02). The expression of CAR and 18S rRNA was determined using qPCR with following primer sets:

CAR-For: 5'-GACGCTCTTCACATGCAGG-3'

CAR-Rev: 5'-GAGAAGCATCTAGGGCCG-3'

CAR-Prob: 5'-VIC-GGAGAGGGCAGAGGA-3'

18S rRNA For: 5'-ATCAGATACCGTCGTAGTTCCG-3'

18S rRNA Rev: 5'-GCCCTTCCGTCAATTCCTTTAAG-3'

18S rRNA MGB probe: 5'-VIC-CCATAAACGATGCCGACCGGCG-3'

Surface density of CAR molecules

The number of CAR molecules on the CAR-T cell surface was quantitated using Quantum Simply Cellular (QSC) (Bangs Laboratories, USA: 815), which allows for the conversion of the cell fluorescence intensity value into absolute numbers of binding molecules using a calibration curve. The absolute number and MFI were calculated using

QUICKCAL version 2.3 according to the manufacturer's instructions. Data acquisition was performed on a MACSquant 10, and the results were analyzed using FlowJo Software version 10 (Tree Star).

Raji xenograft mouse model

Six- to 8-week-old male NOD/SCID mice were engrafted with 1×10^6 Raji/ffluc cells via tail vein injection. Three days later, CAR-T or control T cells that had been expanded for 14 days were injected via the tail vein. The number of injected cells was adjusted according to the transduction rate. Animal weights were monitored twice weekly. Tumor progression was evaluated by BLI using a Xenogen IVIS LUMINA III *In Vivo* Imaging System (PerkinElmer) for up to 28 days.

Subject enrollment and preconditioning

All enrolled subjects were informed and consented to this trial. A conventional fludarabine/cyclophosphamide (F/C) regimen was used for lymphodepletion (F: 30 mg/m² day -5 to day -3; C: 250 mg/m² from day -5 to day -3). Subjects were infused with 3×10^5 CAR-T cells/kg. One subject in the EF1A19 group was excluded from the trial due to the clearance of bone marrow blasts by the preconditioning F/C regimen. The severity of CRS was graded according to the Penn system.³⁰ Neurological toxicities were graded according to the National Cancer Institute Common Toxicity Criteria for Adverse Events (NCI CTCAE; version 4.03).³¹

Statistics

Statistical analyses were performed in GraphPad Prism version 8.02. Because the sample size of subjects was small and the most of this study was descriptive, we used descriptive statistics (mean and standard deviation or median and range) to summarize the data. Analyses of the *in vivo* BLI of tumors were performed using two-way ANOVA with repeated measures. The significance of the findings was defined as follows: ns, not significant, $p > 0.05$; * $p < 0.05$; ** $p < 0.01$; and *** $p < 0.001$.

SUPPLEMENTAL INFORMATION

Supplemental information can be found online at <https://doi.org/10.1016/j.omtm.2021.03.007>.

ACKNOWLEDGMENTS

We thank the patients and their families for their understanding and participation. This study was supported by Natural Science Foundation of Hebei Province, China H2019B72003, Science and Technology Bureau of Shijiazhuang, China 198200047A, and Department of Science and Technology of Hebei Province, China 199A2406H. The material and sequences may be obtained by emailing lijianqiang@senlangbio.com.

AUTHOR CONTRIBUTIONS

Conceptualization, J.L. and J.H.; methodology, J.L. and J.H.; investigation, L.W., Y.L., and M.B.; writing – original draft, J.H.; writing – review & editing, J.L. and J.H.; funding acquisition, J.L. and J.H.; resources, J.Y., X.Z., and P.L.; supervision, J.L. and P.L.

DECLARATION OF INTERESTS

J.L. is the founder of Hebei Senlang Biotechnology, Co. The remaining authors declare no competing interests.

REFERENCES

- Kochenderfer, J., Somerville, R., Lu, T., Shi, V., Yang, J.C., Sherry, R., Klebanoff, C., Kammula, U.S., Goff, S.L., Bot, A., et al. (2016). Anti-CD19 chimeric antigen receptor T cells preceded by low-dose chemotherapy to induce remissions of advanced lymphoma. *J. Clin. Oncol.* 34, LBA3010.
- Park, J.H., Rivière, I., Gonen, M., Wang, X., Sénéchal, B., Curran, K.J., Sauter, C., Wang, Y., Santomasso, B., Mead, E., et al. (2018). Long-Term Follow-up of CD19 CAR Therapy in Acute Lymphoblastic Leukemia. *N. Engl. J. Med.* 378, 449–459.
- Maude, S.L., Laetsch, T.W., Buechner, J., Rives, S., Boyer, M., Bittencourt, H., Bader, P., Verneer, M.R., Stefanski, H.E., Myers, G.D., et al. (2018). Tisagenlecleucel in Children and Young Adults with B-Cell Lymphoblastic Leukemia. *N. Engl. J. Med.* 378, 439–448.
- Kochenderfer, J.N., Somerville, R.P.T., Lu, T., Yang, J.C., Sherry, R.M., Feldman, S.A., McIntyre, L., Bot, A., Rossi, J., Lam, N., and Rosenberg, S.A. (2017). Long-Duration Complete Remissions of Diffuse Large B Cell Lymphoma after Anti-CD19 Chimeric Antigen Receptor T Cell Therapy. *Mol. Ther.* 25, 2245–2253.
- Brudno, J.N., and Kochenderfer, J.N. (2018). Chimeric antigen receptor T-cell therapies for lymphoma. *Nat. Rev. Clin. Oncol.* 15, 31–46.
- Schuster, S.J., Bishop, M.R., Tam, C.S., Waller, E.K., Borchmann, P., McGuirk, J.P., Jäger, U., Jaglowski, S., Andreadis, C., Westin, J.R., et al.; JULIET Investigators (2019). Tisagenlecleucel in Adult Relapsed or Refractory Diffuse Large B-Cell Lymphoma. *N. Engl. J. Med.* 380, 45–56.
- Mahadeo, K.M., Khazal, S.J., Abdel-Azim, H., Fitzgerald, J.C., Taraseviciute, A., Bollard, C.M., Tewari, P., Duncan, C., Traube, C., McCall, D., et al.; Pediatric Acute Lung Injury and Sepsis Investigators (PALISI) Network (2019). Management guidelines for paediatric patients receiving chimeric antigen receptor T cell therapy. *Nat. Rev. Clin. Oncol.* 16, 45–63.
- Yu, S., Yi, M., Qin, S., and Wu, K. (2019). Next generation chimeric antigen receptor T cells: safety strategies to overcome toxicity. *Mol. Cancer* 18, 125.
- Ghorashian, S., Kramer, A.M., Onuoha, S., Wright, G., Bartram, J., Richardson, R., Albon, S.J., Casanovas-Company, J., Castro, F., Popova, B., et al. (2019). Enhanced CAR T cell expansion and prolonged persistence in pediatric patients with ALL treated with a low-affinity CD19 CAR. *Nat. Med.* 25, 1408–1414.
- Fry, T.J., Shah, N.N., Orentas, R.J., Stetler-Stevenson, M., Yuan, C.M., Ramakrishna, S., Wolters, P., Martin, S., Delbrook, C., Yates, B., et al. (2018). CD22-targeted CAR T cells induce remission in B-ALL that is naive or resistant to CD19-targeted CAR immunotherapy. *Nat. Med.* 24, 20–28.
- Yañez, L., Sánchez-Escamilla, M., and Perales, M.-A. (2019). CAR T Cell Toxicity: Current Management and Future Directions. *HemaSphere* 3, e186.
- Rice, J., Nagle, S., Randall, J., and Hinson, H.E. (2019). Chimeric Antigen Receptor T Cell-Related Neurotoxicity: Mechanisms, Clinical Presentation, and Approach to Treatment. *Curr. Treat. Options Neurol.* 21, 40.
- Watanabe, K., Terakura, S., Martens, A.C., van Meerten, T., Uchiyama, S., Imai, M., Sakemura, R., Goto, T., Hanajiri, R., Imahashi, N., et al. (2015). Target antigen density governs the efficacy of anti-CD20-CD28-CD3 ζ chimeric antigen receptor-modified effector CD8+ T cells. *J. Immunol.* 194, 911–920.
- Rad S M, A.H., Poudel, A., Tan, G.M.Y., and McLellan, A.D. (2020). Promoter choice: Who should drive the CAR in T cells? *PLoS ONE* 15, e0232915.
- Robbins, P.B., Yu, X.J., Skelton, D.M., Pepper, K.A., Wasserman, R.M., Zhu, L., and Kohn, D.B. (1997). Increased probability of expression from modified retroviral vectors in embryonal stem cells and embryonal carcinoma cells. *J. Virol.* 71, 9466–9474.
- Robbins, P.B., Skelton, D.C., Yu, X.-J., Halene, S., Leonard, E.H., and Kohn, D.B. (1998). Consistent, persistent expression from modified retroviral vectors in murine hematopoietic stem cells. *Proc. Natl. Acad. Sci. USA* 95, 10182–10187.
- Halene, S., Wang, L., Cooper, R.M., Bockstoe, D.C., Robbins, P.B., and Kohn, D.B. (1999). Improved expression in hematopoietic and lymphoid cells in mice after transplantation of bone marrow transduced with a modified retroviral vector. *Blood* 94, 3349–3357.

18. Astrakhan, A., Sather, B.D., Ryu, B.Y., Khim, S., Singh, S., Humblet-Baron, S., Ochs, H.D., Miao, C.H., and Rawlings, D.J. (2012). Ubiquitous high-level gene expression in hematopoietic lineages provides effective lentiviral gene therapy of murine Wiskott-Aldrich syndrome. *Blood* *119*, 4395–4407.
19. Singh, S., Khan, L., Khim, S., Seymour, B., Sommer, K., Wielgosz, M., Norgaard, Z., Kiem, H.-P., Adair, J., Liggitt, D., et al. (2016). Safe and Effective Gene Therapy for Murine Wiskott-Aldrich Syndrome Using an Insulated Lentiviral Vector. *Mol. Ther. Methods Clin. Dev.* *4*, 1–16.
20. Gerby, B., Armstrong, F., de la Grange, P.B., Medyouf, H., Calvo, J., Verhoeyen, E., Cosset, F.L., Bernstein, I., Amselem, S., Boissel, N., et al. (2010). Optimized gene transfer into human primary leukemic T cell with NOD-SCID/leukemia-initiating cell activity. *Leukemia* *24*, 646–649.
21. Chan, W.K., Suwannasaen, D., Throm, R.E., Li, Y., Eldridge, P.W., Houston, J., Gray, J.T., Pui, C.H., and Leung, W. (2015). Chimeric antigen receptor-redirected CD45RA-negative T cells have potent antileukemia and pathogen memory response without graft-versus-host activity. *Leukemia* *29*, 387–395.
22. Wang, X., Chang, W.-C., Wong, C.W., Colcher, D., Sherman, M., Ostberg, J.R., Forman, S.J., Riddell, S.R., and Jensen, M.C. (2011). A transgene-encoded cell surface polypeptide for selection, in vivo tracking, and ablation of engineered cells. *Blood* *118*, 1255–1263.
23. Quadrini, K.J., Hegelund, A.C., Cortes, K.E., Xue, C., Kennelly, S.M., Ji, H., Högerkorp, C.-M., and Mc Closkey, T.W. (2016). Validation of a flow cytometry-based assay to assess C5aR receptor occupancy on neutrophils and monocytes for use in drug development. *Cytometry B Clin. Cytom.* *90*, 177–190.
24. MacLeod, D.T., Antony, J., Martin, A.J., Moser, R.J., Hekele, A., Wetzel, K.J., Brown, A.E., Triggiano, M.A., Hux, J.A., Pham, C.D., et al. (2017). Integration of a CD19 CAR into the TCR Alpha Chain Locus Streamlines Production of Allogeneic Gene-Edited CAR T Cells. *Mol. Ther.* *25*, 949–961.
25. Eyquem, J., Mansilla-Soto, J., Giavridis, T., van der Stegen, S.J.C., Hamieh, M., Cunanan, K.M., Odak, A., Gönen, M., and Sadelain, M. (2017). Targeting a CAR to the TRAC locus with CRISPR/Cas9 enhances tumour rejection. *Nature* *543*, 113–117.
26. Guedan, S., Posey, A.D., Jr., Shaw, C., Wing, A., Da, T., Patel, P.R., McGettigan, S.E., Casado-Medrano, V., Kawalekar, O.U., Uribe-Herranz, M., et al. (2018). Enhancing CAR T cell persistence through ICOS and 4-1BB costimulation. *JCI Insight* *3*, e96976.
27. Liu, Z., Chen, O., Wall, J.B.J., Zheng, M., Zhou, Y., Wang, L., Vaseghi, H.R., Qian, L., and Liu, J. (2017). Systematic comparison of 2A peptides for cloning multi-genes in a polycistronic vector. *Sci. Rep.* *7*, 2193.
28. Carreno, B.M., Garbow, J.R., Kolar, G.R., Jackson, E.N., Engelbach, J.A., Becker-Hapak, M., Carayannopoulos, L.N., Piwnica-Worms, D., and Linette, G.P. (2009). Immunodeficient mouse strains display marked variability in growth of human melanoma lung metastases. *Clin. Cancer Res.* *15*, 3277–3286.
29. Ma, F., Ho, J.-Y., Du, H., Xuan, F., Wu, X., Wang, Q., Wang, L., Liu, Y., Ba, M., Wang, Y., et al. (2019). Evidence of long-lasting anti-CD19 activity of engrafted CD19 chimeric antigen receptor-modified T cells in a phase I study targeting pediatrics with acute lymphoblastic leukemia. *Hematol. Oncol.* *37*, 601–608.
30. Porter, D., Frey, N., Wood, P.A., Weng, Y., and Grupp, S.A. (2018). Grading of cytokine release syndrome associated with the CAR T cell therapy tisagenlecleucel. *J. Hematol. Oncol.* *11*, 35.
31. Neelapu, S.S., Tummala, S., Kebriaei, P., Wierda, W., Gutierrez, C., Locke, F.L., Komanduri, K.V., Lin, Y., Jain, N., Daver, N., et al. (2018). Chimeric antigen receptor T-cell therapy - assessment and management of toxicities. *Nat. Rev. Clin. Oncol.* *15*, 47–62.